Iranica Journal of Energy & Environment 4 (4): 376-384, 2013
ISSN 2079-2115
IJEE an Official Peer Reviewed Journal of Babol Noshirvani University of Technology
DOI: 10.5829/idosi.ijee.2013.04.04.9

BUT

Mix Convection Heat Transfer in a Lid Driven Enclosure Filled by Nanofluid

H. Hassanzadeh Afrouzi and M. Farhadi

Faculty of Mechanical Engineering, Babol University of Technology, Babol, Iran

(Received: Sep 7, 2013; Accepted in Revised Form: Nov 16, 2013)

Abstract: In the present study, mixed convection flow was investigated by Lattice Boltzmann method in a square lid-driven cavity utilizing nanofluid in presence of cubic obstacle. The fluid in the cavity was a water-based nanofluid containing Cu nanoparticles. The study was carried out for a constant Rayleigh number 10^4, the Richardson number ranging from 0.1 to 10 and the solid volume fraction ranging from 0 to 0.03. The effects of solid concentrations on hydrodynamic and thermal characteristics were investigated. The results were presented in the form of streamlines and temperature contours for different values of solid volume fractions and Richardson numbers. The results indicated that the averaged Nusselt number increases byaugmentation of solid volume fraction. The Richardson number had more effect on Nusselt number when obstacle was located at the bottom section of enclosure.

Keyword: Lattice Boltzmann method · Nanofluid · Mixed convection · Lid driven cavity · Richardson number

INTRODUCTION

The lid-driven cavity problem has been extensively used as a benchmark case for evaluation of numerical solution algorithms [1-4]. Moallemi and Jang [5] have studied the effect of Prandtl number and Reynolds number on the flow and thermal characteristics in a rectangular cavity. Experimental results have been reported by Prasad and Koseff [6] on mixed convection process in a cavity for a different Richardson number ranging from 0.1 to 1000. Rahnama and Farhadi [7] studied the effect of radial fins on turbulent natural convection in an annulus. The effect of fin numbers and length were investigated over the heat transfer. Leong *et al*. [8] have studied heat transfer in a mixed convection open cavity subjected to an external flow. The Reynolds and Grashof numbers and aspect ratio were varied from 1 to 2000, 0 to 10^6 and 0.5 to 4, respectively. Darzi *et al* [9] have investigated the effect of the fins on mixed convection in lid driven cavity for various Richardson number and different height and number of fins. They found that heat transfer enhancement occurs in low fin height and high Richardson number. In recent years, nanofluids have attracted more attention for cooling in various industrial applications because of remarkable increase in effective thermal conductivity of base fluid. Masuda *et al*. [10] have reported on enhanced thermal conductivity of dispersed ultra-fine (nano size) particles in liquids. Soon thereafter, Choi [11] was the first to coin the term "nanofluids" for this new class of fluids with superior thermal properties. Khanafer *et al*. [12] have investigated the heat transfer enhancement in a two-dimensional enclosure utilizing nanofluids for a range of Grashof numbers and volume fractions. It was found that the heat transfer across the enclosure was found to increase with the volumetric fraction of the copper nanoparticles in water for different Grashof number. Jou and Tzeng [13] have conducted a numerical attempt to simulate the natural convection in a rectangular cavity with two different aspect ratios for just Cu-water nanofluid. They simulated the flow field in aspect ratios where the convection heat transfer is dominant than conduction heat transfer, but they didn't report the details of heat transfer enhancement. Talebi *et al*. [14] have demonstrated a numerical study of laminar mixed convection through copper-water nanofluid in square cavity for different Reynolds and Rayleigh numbers.

One of the suitable methods that have been used in the recent years is the Lattice Boltzmann method. It was used for simulation of the flow field and thermal

Corresponding Author: H. Hassanzadeh Afrouzi, Faculty of Mechanical Engineering, Babol University of Technology, Babol, Iran. E-mail: hamidhasanzade@yahoo.com.

characterization in the field of engineering applications [15-17], entropy generation [18], porous media [19], multiphase flow [20] and etc. LBM has ability to simulate complex flow such as micro channel [21, 22] and fuel cell [23, 24].

In the present study LBM approach is used to simulate mixed convection flow utilizing nanofluids in a square lid-driven cavity with presence of cubic obstacle. Finally the local and averaged Nusselt numbers, streamlines, temperature contours for different values of solid volume fraction, Richardson numbers and obstacle positions are illustrated.

Numerical Procedure

Lattice Boltzmann Method: The thermal LB model utilizes two distribution functions, f and g, for the flow and temperature fields, respectively. It uses modeling of movement of fluid particles to capture macroscopic fluid quantities such as velocity, pressure and temperature. In this approach the fluid domain is discretized in uniform Cartesian cells. Each cell holds a fixed number of distribution functions, which represent the number of fluid particles moving in these discrete directions. For this work the D2Q9 model has been used. The values of w_o = 4/9 for $|c_{1\text{-}4}| = 1$ (for the static particle), $w_{5\text{-}9}$ for $|c| = \sqrt{2}$ and f for g, are assigned in this model. The density and distribution functions i.e. the f and g, are calculated by solving the Lattice Boltzmann equation (LBE), which is a special discretization of the kinetic Boltzmann equation. After introducing BGK approximation, the general form of lattice Boltzmann equation with external force can be written as [9]:

For the Flow Field:

$$f(x + c\Delta t, t + \Delta t) = f(x,t) + \frac{\Delta t}{\tau}[f(x,t) - f(x,t)] + \Delta t c F \quad (1)$$

For the Temperature Field:

$$g(x + c\Delta t, t + \Delta t) = g(x,t) + \frac{\Delta t}{\tau}[g(x,t) - g(x,t)] \quad (2)$$

Where Δt denotes lattice time step, c_k is the discrete lattice velocity in direction k, F_k is the external force in direction of lattice velocity, τ_v and τ_D denotes the lattice relaxation time for the flow and temperature fields. The kinetic viscosity υ and the thermal diffusivity α, are defined in terms of their respective relaxation times, i.e. $\upsilon = c(\tau - 1/2)$ and $\alpha = c(\tau - 1/2)$, respectively. Note that the limitation $0.5 < \tau$ should be satisfied for both relaxation times to ensure that viscosity and thermal diffusivity are positive. Furthermore, the local equilibrium distribution function determines the type of problem that needs to be solved. It also models the equilibrium distribution functions, which are calculated with Eq. (3) and Eq. (4) for flow and temperature fields, respectively [14].

$$f = w\rho[1 + \frac{c.u}{c} + \frac{1}{2}\frac{(c.u)}{c} - \frac{1}{2}\frac{u}{c}] \quad (3)$$

$$g = wT[1 + \frac{c.u}{c}] \quad (4)$$

Where w_k is a weighting factor, ρ is the lattice fluid density. In order to incorporate buoyancy force in the model, the force term in the Eq. (1) need to be calculated as below in vertical direction (y):

$$F = 3wg\beta\theta \quad (5)$$

For natural convection the Boussinesq approximation is applied and radiation heat transfer is negligible. To ensure that the code works in near incompressible regime, the characteristic velocity of the flow for both natural $(V = \sqrt{\beta g \Delta T H})$ and force $(V = \mathrm{Re}\upsilon / H)$ regimes must be small compared to the fluid speed of sound. In the present study, the characteristic velocity was selected as 0.1 of sound speed.Finally, macroscopic variable can be calculated in terms of these variables, with the following formulas for flow density, momentum and temperature, respectively [15].

$$\rho = \sum_k f_k$$
$$\rho u_i = \sum_k f_k c_{ki} \quad (6)$$
$$T = \sum_k g_k$$

Lattice Boltzmann Model for Nanofluid: In order to simulate the nanofluid by the lattice Boltzmann method, Because of the inter particle potentials and other forces on the nanoparticles, the nanofluid behaves differently from the pure liquid from the mesoscopic point of view and is of high efficiency in energy transport as well as desired stabilization than the common solid-liquid mixture. For pure fluid in absence of nanoparticles in the cavity, the governed equations are Eqs. (1-6). However, for modeling the nanofluid because of changing in the fluid thermal conductivity, density, heat capacitance and thermal expansion, some of the governed equations should be changed. The thermal diffusivity is written as [17]:

$$\alpha_{nf} = \frac{k_{nf}}{(\rho c_p)_{nf}} \tag{7}$$

The effective density of nanofluid is defined as [17]:

$$\rho_{nf} = (1-\phi)\rho_f + \phi\rho_s \tag{8}$$

Whereas the heat capacitance of the nanofluid and part of the Boussinesq term are [17]:

$$(\rho c_p)_{nf} = (1-\phi)(\rho c_p)_f + \phi(\rho c_p)_s \tag{9}$$

$$(\rho\beta)_{nf} = (1-\phi)(\rho\beta)_f + \phi(\rho\beta)_s \tag{10}$$

With ϕ being the volume fraction of the solid particles and subscripts *f*, *nf* and *s* stand for base fluid, nanofluid and solid particle, respectively. The effective viscosity of nanofluid was introduced by Brinkman [25] as Eq. (11).

$$\mu_{eff} = \frac{\mu_f}{(1-\phi)^{2.5}} \tag{11}$$

The effective thermal conductivity of nanofluid was given by Patel *et al*. [26] as Eq. (12).

$$k_{eff} = k_f + k_p\frac{A_p}{A_f} + ck_pPe\frac{A_p}{A_f} \tag{12}$$

Where c is constant and must be determined experimentally, A_P / A_f and Pe here is defined as:

$$\frac{A_p}{A_f} = \frac{d_p}{d_f}\frac{\phi}{(1-\phi)} \tag{13}$$

$$Pe = \frac{u_p d_p}{\alpha} \tag{14}$$

Where $d_p$is solid particles diameter that is assumed to be equal to 100 nm in this study, $d_f$is the molecular size of liquid that is taken as 2Å for water. The Brownian motion velocity is defined as [14]:

$$u_p = \frac{2k_bT}{\pi\mu_f d_p^2} \tag{15}$$

Where c is Boltzmann constant. The local and average Nusselt numbers are defined as follows:

$$Nu_l = \frac{k_{eff}}{k_f}\frac{\partial\theta}{\partial n}\bigg|_{n=0} \tag{16}$$

$$Nu_{avg} = \frac{1}{L}\int_0^L Nu_l\, dl \tag{17}$$

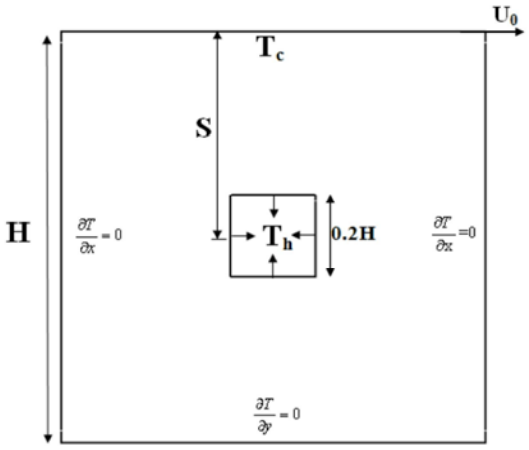

Fig. 1: Computational domain of present study.

Table 1: Thermo physical properties of base fluid and nanoparticles

Property	Water	Copper
ρ(kg/m3)	997.1	8954
C_p(J/kg.K)	4179	383
k(W/m.K)	0.6	400
β(1/K)	2.1×10^{-4}	1.67×10^{-5}

Where L is the length of obstacle.è is dimensionless temperature and it is calculated as:

$$\theta = \frac{T-T_c}{T_h-T_c} \tag{18}$$

The dimensionless relaxation time for velocity and thermal fields which are determined by the nanofluid properties as follows [15]:

$$\tau_v = \frac{3}{2}\frac{\upsilon_{nf(lbm)}}{c^2\delta t} + 0.5 = \frac{3}{2}\frac{\mu_{nf(lbm)}}{\rho_{nf(lbm)}c^2\delta t} + 0.5 \tag{19}$$

$$\tau_D = \frac{3}{2}\frac{\alpha_{nf(lbm)}}{c^2\delta t} + 0.5 = \frac{3}{2}\frac{k_{nf(lbm)}}{(\rho c_p)_{nf(lbm)}c^2\delta t} + 0.5 \tag{20}$$

That *lbm* subscript determines the lattice scale. This procedure is the same as Das *et al*. [27] and Wang et.al [28].

Computational Domain: In the simulation of model, the flow is assumed steady, two dimensional, incompressible and laminar. The computational domain is considered a lid driven cavity with a square obstacle which located at the center of cavity (Figure 1).

Square side is 0.2 as cavity side. The distance of square center from the floor of the cavity ranges from 0.25H to 0.75H. All cavity walls are adiabatic except the

top cold wall (T_c) and the obstacle is maintained at constant high temperature (T_h). The properties of copper nano particles and water as base fluid are given in Table 1.

RESULTS AND DISCUSSION

Mix convection flow of the 0 to 0.03 cu-water nanofluid was investigated in a cubic with the presence of a hot square obstacle in different vertical sections and Ri numbers. The dimensionless vertical position and Richardson number,Riranges from 0.25 to 0.75 and 0.1 to 10, respectively.The effect of the vertical position of heated hollow obstacle is examined using the numerical scheme of Lattice Boltzmann Method. The fluid flow and heat transfer characteristics in the present study depend on parameters like lid velocity, Richardson number (Ri), Prandtl number (Pr), dimensionless cylinder position (S^*) and nanoparticles volume fraction (ϕ). A number of governing dimensionless parameters are required to characterize the system. Therefore, a comprehensive analysis of all combinations of parameters is not practical. The objective of this paper is to investigate the effects of S^*, Ri and ϕ on the flow structure and convective heat transfer in the lid driven enclosure. At constant Pr value of 6.2 and Re of 100, dimensionless obstacle position (S^*), Richardson number (Ri) and nanoparticles volume fraction (ϕ) vary between 0.25 to 0.75, 0.1 to 10 and 0 to 0.03, respectively. For validation of nanofluid behavior, the natural convection in an enclosure filled with Cu-water is simulated and temperature profile on axial midline is compared to the results of Khanafer *et al*. [12] as shown in Figure 2. For further validation, mixed convection is simulated in a lid driven cavity which is filled with nanofluid and average Nusselt number is compared with Talebi *et al*. [11] (Figure 3). Results showed a good agreement with theoretical concept. To study the mesh independency, the average Nusselt number on the hot obstacle was chose for case with Ri=0.1 and S^*=0.75 (Table 2). The mesh resolution of 200×200 was selected for all cases in accordance with the obtained results.

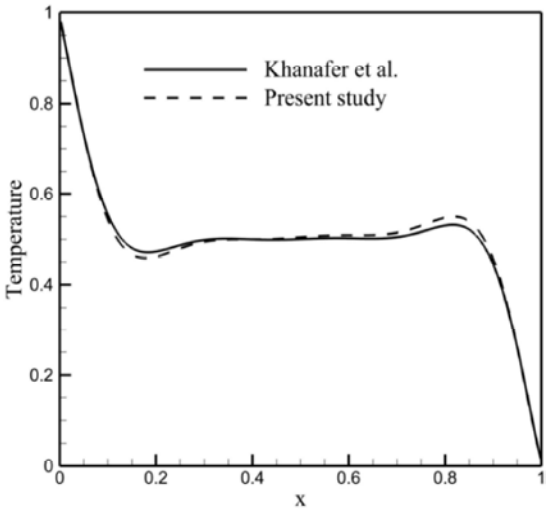

Fig. 2: Temperature profile on axial midline for the case of $Ra = 1.98 \times 10^5$,Pr=0.71 and Comparison with numerical results by Khanafer *et al.* [12].

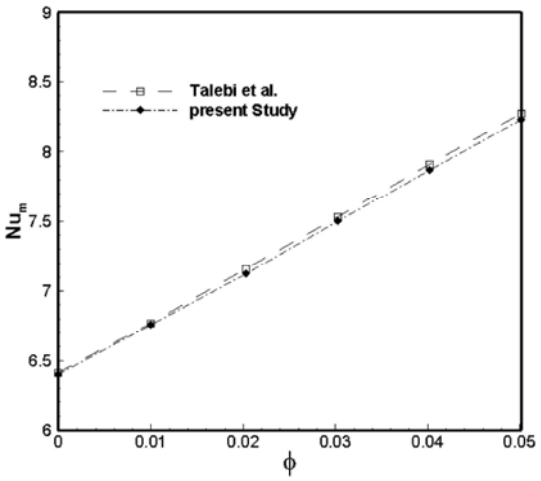

Fig. 3: Comparison of the average Nusselt number along hot surface between present study and Talebi et al. [14] at Re=100, Ra=1.47×10^5

Table 2: Study of solution sensitivity to number of grids

Number of grids	Averaged Nusselt number on hot surfaces for S=0.75 and Ri=0.1	Diff(%)
100×100	3.005	-
150×150	3.245	7.98
200×200	3.411	5.11
250×250	3.473	1.82

Flow Field: As shown in Figure 4, there is a recirculation zone in the right side of obstacle for all Richardson number when obstacle was located at the top section of the enclosure (S^*=0.25). Top lid movement had more effect on the flow field when force convection is dominant so that recirculation zone extended to bottom of the obstacle, whereas recirculation zone limited to right side of obstacle as Richardson number increased (the effect of the natural convection raised). Figure 5 shows that recirculation zone formed at the left-top side of the obstacle, when hot obstacle located at the center of the cavity (S^*=0.5). This zone enlarges because of natural convection effect when Richardson number increased. Also this region

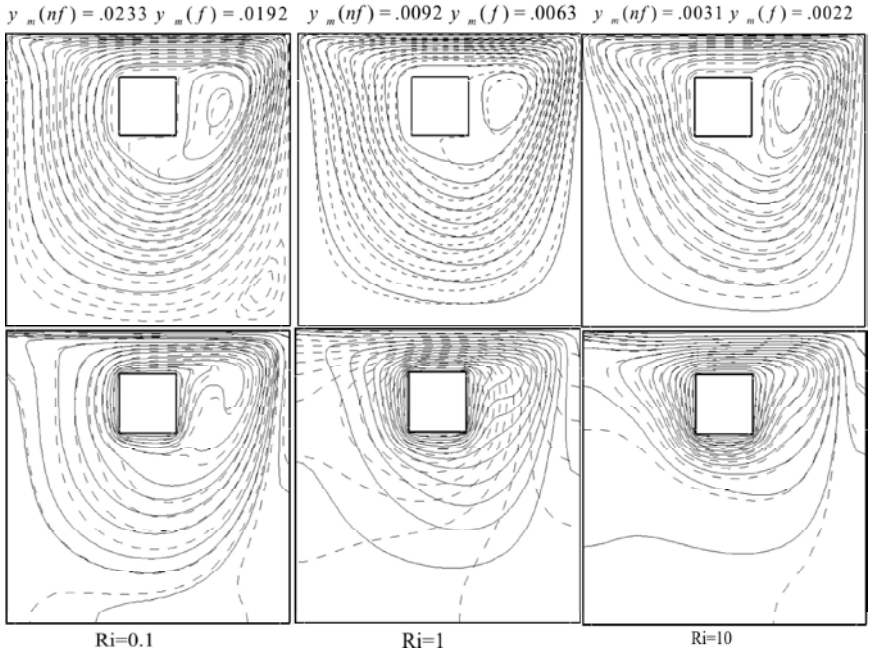

Fig. 4: Streamlines and isotherms for S^*=0.25: line($\phi = 0.03$), dashed line($\phi = 0$)

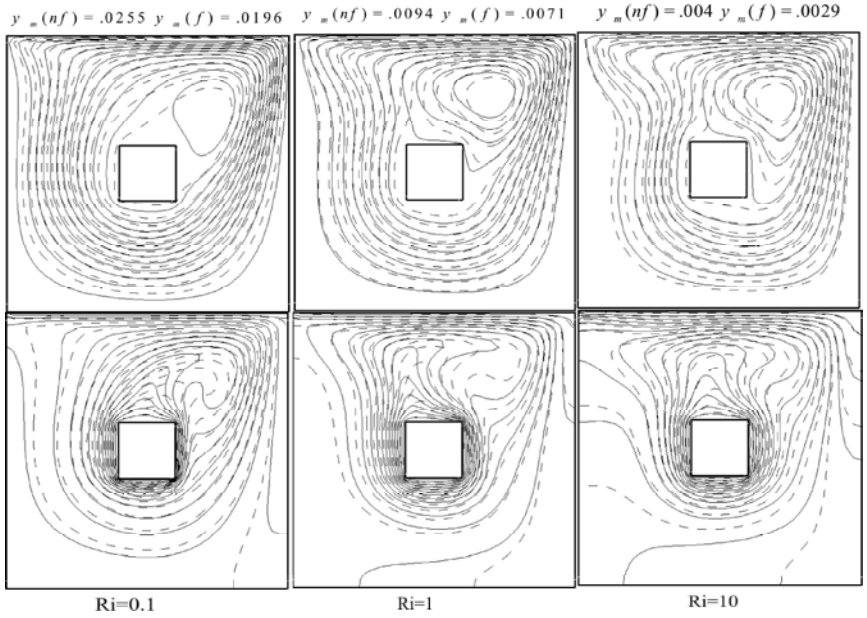

Fig. 5: Streamlines and isotherms for S^*=0.5: line ($\phi = 0.03$), dashed line ($\phi = 0$)

enlarged when Nano-particle volume fraction increased for all Richardson numbers. As shown in Figure6 large space between top moving lid and obstacle led to recirculation zone above the hot obstacle filled almost their whole inter space a tS^*=0.75. The center of this recirculation zone moves to the center of this region as natural convection effect increased.

Temperature: Figure 4 showed that when hot obstacle located at the top section of the enclosure(S^*=0.25) boundary layer rises at the right side of obstacle where recirculation zone have formed. For Ri=0.1 where force convection dominated, isotherms at the left side formed in vicinity of the obstacle. Growth of natural convection moves these lines to the left at larger Richardson number.

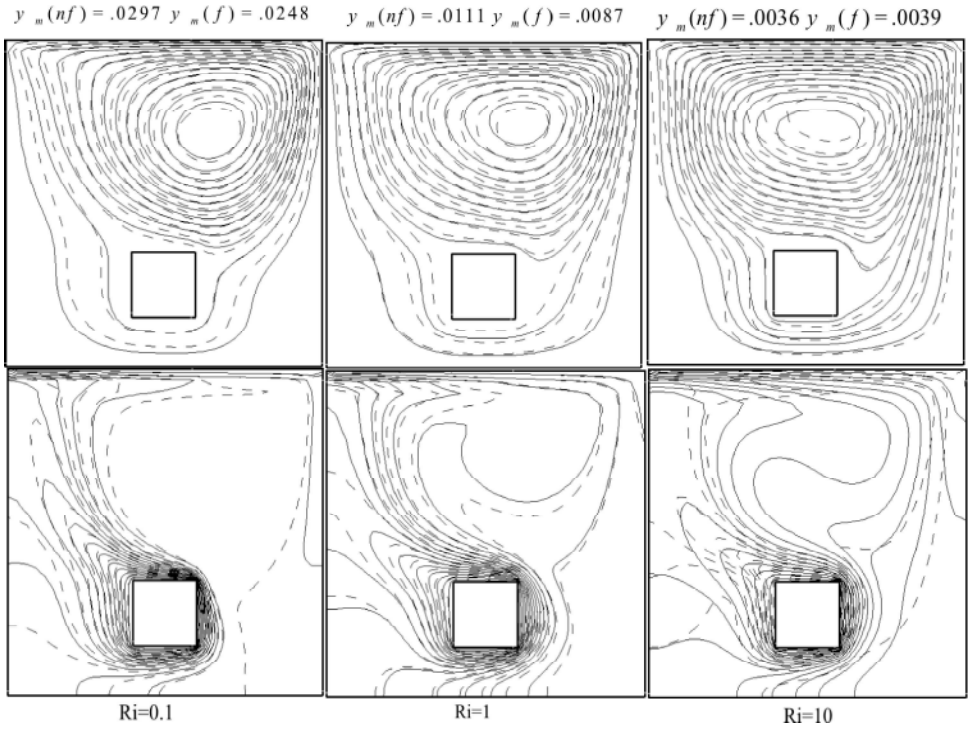

Fig. 6: Streamlines and Isotherms for S*=0.75: line ($\phi = 0$) , dashed line ($\phi = 0.03$)

Another effect of increasing natural convection effect was to make recirculation power weaker that caused decreasing of recirculation zone effect on the isotherms lines. Because of the presence of the hot top wall natural convection weakened and so isotherm lines between bottom surface of obstacle and bottom wall of cavity aggregate near the obstacle bottom surfaceas Richardson number increased.

When hot obstacle moves to downward no considerable change occurs on the isotherm lines by increasing Richardson number. This changeless was distinct for Richardson number augmentation from 1 to 10 (Figures 5 and 6). When obstacle located at the center of the cavity, symmetrization of isotherm lines overhead the obstacle, by increasing Richardson number, demonstrated that in this region dominant heat transfer mechanism changed from force convection to natural one (Figure 5). By locating hot obstacle at the bottom section of the enclosure as shown in Figure 6 big recirculation zone brought cold fluid toward the hot obstacle. This large zone caused hot surfaces affected on the large amount of flow. So boundary layer grows up at the corner at which this recirculation zone did not extend. However this effect weakened due to diminish of recirculation power as natural effect increased at bigger Richardson number.

The local Nusselt number on the hot surfaces of obstacle that has shown in Figure 7 indicated the heat transfer from each grid at the hot surfaces. It is clear that the local Nusselt number has maximum value on the hot surfaces which has better contact with cold flow. It was predictable that in each case local Nusselt was maximum at the zone in which cold water contacted to the hot surface. By Locating hot obstacle in the bottom section of the cavity at Ri=0.1 the start point of the obstacle that touched the recirculation zone (d) had maximum Nusselt number. Cold water contacted the upper surface of obstacle and led to increase local Nusselt number at this surface. At higher Richardson number as natural effect increase, local Nusselt number at all surfaces were almost equal. When obstacle located at the center and force convection dominating (Ri=0.1), upper cold water reached the obstacle at point c. at that position top and right surfaces of obstacle had least Nusselt number because of recirculation zone presence. And maximum heat transfer accrued on the c-d and b-c surfaces for Richardson number 1 and 10. Finally the maximum local Nusselt number reached for S^*=0.75 where a large amount of cold water could contact the hot obstacle. Top and left surfaces of obstacle (d-a, a-b) had greatest heat transfer rate at Ri=0.1. At Ri=1 where mix convection existed left,

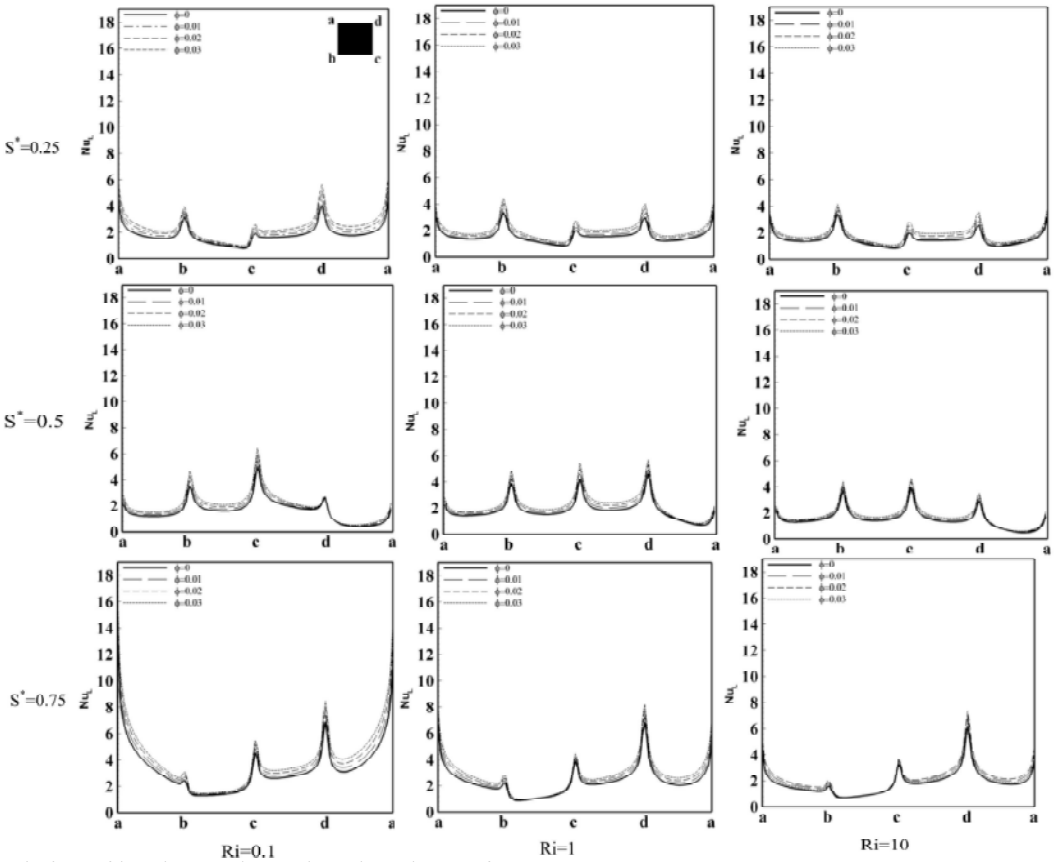

Fig. 7: Variation of local Nusselt number along hot surfaces

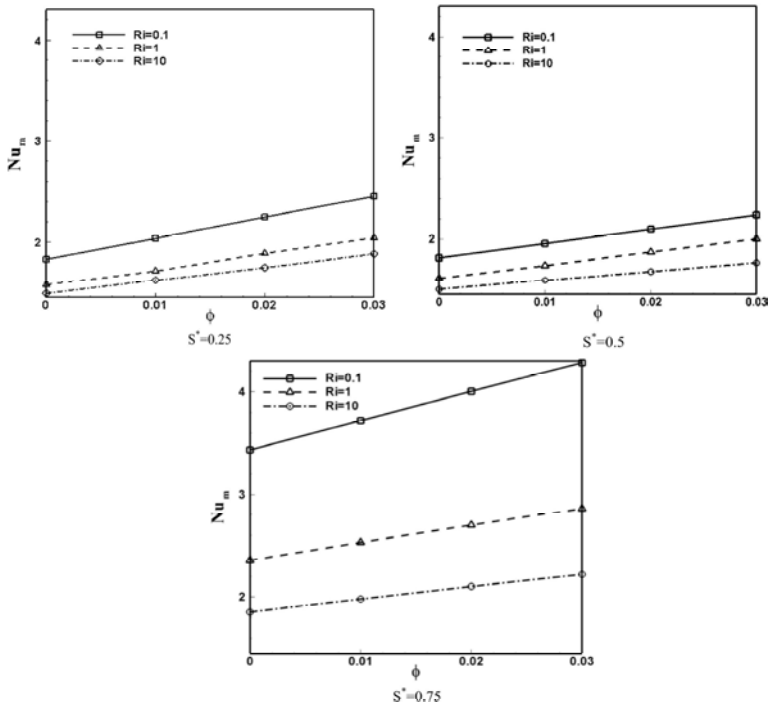

Fig. 8: Variation of average Nusselt number over the hot obstacle surfaces

right and top surfaces were almost equal in heat transfer. For pure natural convection (Ri=10) top and right surfaces had greater local Nusselt number. for (S^*=0.75) at all Richardson number bottom surface of hot obstacle had least Nusselt number that was due to presence of a natural convection region with hot thermal boundary condition at the top.

Figure8 indicated the average Nusselt number versus nano particle volume fraction for different Richardson number. For all hot obstacle positions and Richardson numbers heat transfer increased by increasing of nano particles volume fraction and decreasing of Richardson number.

CONCLUSION

Simulation of nanofluid mix convection was investigated in a square lid driven cavity with the presence of a hot square obstacle by using the Lattice Boltzmann method. The effect of obstacle vertical position, Richardson number and volume fraction of Cu nanoparticles in the range were investigated on mixed convection flow and heat transfer. Results showed that the streamlines have different patterns at different Richardson numbers. The heat transfer rate increases by augmentation of nano particles concentration at constant Richardson number and obstacle vertical position. Also Richardson number is more effect on the flow field, isotherms and Nusselt number when obstacle was located at the bottom section of the enclousure.

REFFERENCE

1. Golkhou, F., M. Tajee and H. Mosavian, 2013. CFD Simulation of Nanosufur Crystallization Incorporating Population Balance Modeling. Iranica Journal of Energy and Environment, 4: 36-42.
2. Sajjadi, B., M. Keshavarz and R. Davarnejad 2011. Investigation of Temperature and Influent Load on Nitrifying Treatment of Using Wastewater CFD. Iranica Journal of Energy and Environment, 2: 08-17.
3. Schreiber, R. and H.B. Keller, 1983. Driven cavity flows by efficient numerical techniques. Journal of Computational Physics, 49(2): 310-333.
4. Iwatsu, R., J.M. Hyun and K. Kuwahara, 1993. Mixed convection in a driven cavity with a stable vertical temperature gradient.International Journal of Heat and Mass Transfer, 36: 1601-1608.
5. Moallemi, M.K. and K.S. Jang, 1992. Prandtl number effects on laminar mixed convection heat transfer in a lid-driven cavity. International Journal of Heat and Mass Transfer, 35: 1881-1892.
6. Prasad, A.K. and J.R. Koseff, 1996. Combined forced and natural convection heat transfer in a deep lid-driven cavity flow. International Journal of Heat and Fluid Flow, 17(5): 460-467.
7. Rahnama, M. and M. Farhadi, 2004. Investigated effect of radial fins on two-dimensional turbulent natural convection in a horizontal annulus. International Journal of Thermal Sciences, 43: 255-264.
8. Leong, J.C., N.M. Brown and F.C. Lai, 2005. Mixed convection from an open cavity in a horizontal channel. International Communications in Heat and Mass Transfer, 32(5): 583-592.
9. Darzi, A.A.R., M. Farhadi and K. Sedighi, Numerical study of the fins effect on mixed convection heat transfer in a lid-driven cavity, Proceedings of the Institution of Mechanical Engineers, Part C: Journal of Mechanical Engineering Science, Article in press.
10. Masuda, H. A. Ebata, K. Teramae and N. Hishinuma, 1993. Alteration of thermal conductivity and viscosity of liquid by dispersing ultra-fine particles. Netsu Bussei, 7: 227-233.
11. Stephen, U.S. Choi and J.A. Eastman, 1995. Enhancing thermal conductivity of fluids with nanoparticles. 1 Energy Technology Division and ^Materials Science Division Argonne National Laboratory, Argonne, IL 6043.
12. Khanafer, K., K. Vafai and M. Lightstone, 2003. Buoyancy-driven heat transfer enhancement in a two-dimensional enclosure utilizing nanofluids, International journal of Heat and Mass Transfer, 46: 3639-3653.
13. Jou, R.Y. and S.C. Tzeng, 2006. Numerical research of nature convective heat transfer enhancement filled with nanofluids in rectangular enclosures. International Communications in Heat and Mass Transfer, 33(6): 727-736.
14. Talebi, F., A.H. Mahmoudi and M. Shahi, 2010. Numerical study of mixed convection flows in a square lid-driven cavity utilizing nanofluid. International Communications in Heat and Mass Transfer, 37(1): 79-90.
15. Hassanzadeh Afrouzi, H. M. Farhadi and A. Abouei Mehrizi, 2013. Numerical simulation of micro particles transport in a concentric annulus by Lattice Boltzmann Method.Advanced Powder Technology, 43(3): 575-584.

16. Rabienataj Darzi, A.A., M. Farhadi, K. Sedighi, E. Fattahi and H. Nemati, 2011. Mixed convection simulation of inclined lid driven cavity using Lattice Boltzmann method. Iranian Journal of Science and Technology Transactions of Mechanical Engineering, 35: 73-83.
17. Nemati, H., M. Farhadi, K. Sedighi, E. Fattahi and A.A.R. Darzi, 2010. Lattice Boltzmann simulation of nanofluid in lid-driven cavity. International Communications in Heat and Mass Transfer, 37(10): 1528-1534.
18. Mehrizi, A.A., M. Farhadi, H.H. Afrouzi, K. Sedighi, A.A. Darzi, 2012.Mixed convection heat transfer in a ventilated cavity with hot obstacle: Effect of nanofluid and outlet port location. International Communications in Heat and Mass Transfer, 39(7): 1000-1008.
19. Mehrizi, A.A., M. Farhadi, K. Sedighi and M.A. Delavar, 2013. Effect of fin position and porosity on heat transfer improvement in a plate porous media heat exchanger. Journal of Taiwan Institute of Chemical Engineering, 44(3): 420-431.
20. Huang, H., Z. Li, S. Liu and X.Y. Lu, 2009. Shan-and-Chen-type multiphase lattice Boltzmann study of viscous coupling effects for two-phase flow in porous media. International Journal for Numerical Methods in Fluids, 61(3): 341-354.
21. Yu, Z., O. Hemminger and L.S. Fan, 2007. Experiment and lattice Boltzmann simulation of two-phase gas-liquid flows in micro channels. Chemical Engineering Science, 62(24): 7172-7183.
22. Alapati, S., S. Kang and Y.K. Suh, 2009. Parallel computation of two-phase flow in a micro channel using the lattice Boltzmann method. Journal of Mechanical Science and Technology, 23: 2492-2501.
23. Hao,L. and P. Cheng, 2010. Lattice Boltzmann simulations of water transport in gas diffusion layer of a polymer electrolyte membrane fuel cell. Journal of Power Sources, 195(12): 3870-3881.
24. Delavar, M.A., M. Farhadi and K. Sedighi, 2010. Numerical simulation of direct methanol fuel cells using lattice Boltzmann method. International Journal of Hydrogen Energy, 35(17): 9306-9317.
25. Brinkman, H.C., 2005.The viscosity of concentrated suspensions and solutions. Journal of Chemical Physics, 20(4): 571-581.
25. Kao, P.H. and R.J. Yang, 2007.Simulating oscillatory flows in Rayleigh Benard convection using the lattice Boltzmann method. International Journal of Heat and Mass Transfer, 50: 3315-3328.
26. Patel, H.E., T. Pradeep, T. Sundararajan, A. Dasgupta, N. Dasgupta and S.K. Das, 2005.A micro convection model for thermal conductivity of nanofluid. Pramana-Journal of Physics, 65(5): 863-869.
27. Das, R., S.C. Mishra and R. Uppaluri, 2009. Retrieval of thermal properties in a transient conduction-radiation problem with variable thermal conductivity. International Journal of Heat and Mass Transfer, 52: 2749-2758.
28. Wang, M., J. Wang, N. Pan and S.H. Chen, 2007. Mesoscopic predictions of the effective thermal conductivity for microscale random porous media. Physical Review, 75(3): 036702, 1-10.

Persian Abstract

چکیده

در مطالعه حاضر جریان جابجایی ترکیبی در یک محفظه مربعی حاوی نانوسیال با وجود یک مانع مربعی توسط روش شبکه‌ی بولتزمن بررسی شده است. نانو سیال داخل محفظه سیال پایه‌ی آب حاوی نانوذرات مس می‌باشد. مطالعه‌ی حاضر در عدد رایلی ثابت $۱۰^{۴}$ و عدد ریچاردسون بین ۰/۱ تا ۱۰ و کسر حجمی نانو ذرات بین ۰ تا ۳ درصد انجام گرفت. تاثیر افزایش غلظت ذرات جامد روی مشخصات حرارتی سیستم اندازه‌گیری شد. نتایج به شکل خطوط جریان و نمایه‌های دما برای کسرهای حجمی نانوذرات و اعداد مختلف ریچاردسون ارائه شدند. نتایج نشان می‌دهد که عدد ناسلت میانگین با افزایش غلظت نانوذرات افزایش پیدا می‌کند. وقتی مانع مربعی در قسمت پایینی مکعب قرار دارد، تغییر عدد ریچاردسون تاثیر بیش‌تری روی انتقال حرارت می‌گذارد.